Jurnal Sains Materi Indonesia
Indonesian Journal of Materials Science

Edisi Khusus Oktober 2007, hal : 46 - 52
ISSN : 1411-1098

Akreditasi LIPI Nomor : 536/D/2007
Tanggal 26 Juni 2007

THE INFLUENCE OF LATTICE STRAIN TO THE CRITICAL CURRENT DENSITY OF YBCO

Engkir Sukirman, Didin S. Winatapura, Wisnu Ari Adi and Yustinus P.
Center for Technology of Nuclear Industry Materials (PTBIN)-BATAN
Kawasan Puspiptek Serpong 15314, Tanggerang

ABSTRACT

THE INFLUENCE OF LATTICE STRAIN TO THE CRITICAL CURRENT DENSITY OF YBCO. The influence of lattice strain to the critical current density of YBCO have been investigated. In this investigation it were prepared the YBCO superconductor samples which made by using a modified melt-textured growth (MMTG) method. The aim of doing this research is to investigate the relation between the critical current density and the lattice strain in YBCO superconductor. The structural and microstructural properties of the samples were characterized by the x-ray diffraction technique. The diffraction data were analyzed by means of a RIETAN software. While, the electrical properties of each samples were characterized by four point probe method. The lattice strains were then determined using the formula : $\langle e^2_{hkl} \rangle = (U - U_o)/32 \ln 2$, where U is the refined FWHM parameters of the broadened peak due to the presence of an inhomogeneous strain field and U_0 is the one due to the instrumental resolution only. The result of analysis indicate that the critical current densities and the lattice strains in YBCO samples have inversed correlation, i.e. when the lattice strain decreases, critical current increases, and conversely. The melt-process through 12 minutes may have possibly eliminated the weak links. Therefore, the critical current density increases, and the lattice strain decreases.

Key words : YBCO, Rietveld method, Lattice strain, Critical current density

ABSTRAK

PENGARUH REGANGAN KISI TERHADAP RAPAT ARUS KRITIS *YBCO*. Pengaruh regangan kisi terhadap rapat arus kritis *YBCO* telah diteliti. Dalam penelitian ini dibuat cuplikan-cuplikan superkonduktor *YBCO* dengan menggunakan metode *MMTG* (*Modified Melt-Textured Growth*). Tujuan penelitian ini adalah menentukan hubungan antara rapat arus kritis dan regangan kisi superkonduktor *YBCO*. Karakteristik struktur dan strukturmikro cuplikan diamati dengan teknik difraksi sinar-x metode analisis *Rietveld*. Sedangkan sifat listrik cuplikan diidentifikasi dengan metode *probe* empat titik. Regangan kisi dihitung menggunakan : $\langle e^2_{hkl} \rangle = (U - U_o)/32 \ln 2$, dimana U dan U_0 adalah parameter *FWHM* hasil penghalusan berturut-turut dari cuplikan *YBCO* dan cuplikan standar Si. Hasil analisis menunjukkan bahwa rapat arus kritis dan regangan kisi memiliki korelasi terbalik; ketika regangan kisi menyusut, maka rapat arus kritis meningkat, dan sebaliknya. Waktu pelelehan hingga 12 menit menyusutkan *weak link* pada superkonduktor *YBCO*, sehingga rapat arus kritis meningkat, dan regangan kisi berkurang.

Kata Kunci : *YBCO*, Metode *Rietveld*, Regangan kisi, Rapat arus kritis

INTRODUCTION

Since the high temperature superconductivity (HTS) discovery in an entirely new class of layered-perovskite, oxygen-sensitive, copper-oxide ceramics by Bednorz and Mueller in early 1986 [1], the research and development on that material still have been going on. There have been many scientific achievements obtained by scientist and technologist throughout the world, including the rigorous application in various field, such as in Sensors, HF Applications, Digital Circuits, Magnets, Power Applications (Power Cable, Fault Current Limiter, Transformers, Generators, Motors, Energy Storage), and Cryocoolers [2].

Oxide superconductors (YBCO [3], BSCCO [4], and TBCCO [5] systems) are among the highly attractive for applications, as they can be made superconductive at liquid nitrogen temperature. For most applications, however, HTS have to fulfill the particular requirements, such as large critical current densities of the order of 10^4 to 10^6 A.cm^{-2} even in the presence of large magnetic fields. Fortunately, critical current density (J_c) is not an intrinsic property of a superconductor and is strongly dependent on its microstructure. Hence, microstructural control is very important in getting the HTS of having large critical current densities.

Although it has been proven that structural control is very difficult in oxide superconductors. Various ways have been performed for the fabrication of bulk HTS, such as sinter and melt processes. Sintering is very common in ceramic processing and has many advantages in making use of conductors. However it has failed in producing high-J_c superconductors [6]. The weak links at grain boundaries are considered as the cause of the low J_c values obtained in sintered bulk samples [7].

Through the melt processes were found that the grains were made to be alignment, and accordingly it reduced the weak links and hence larger J_c values were achieved in YBCO, which is usually called $YBa_2Cu_3O_{7-x}$ compound or 123-phase [8]. However, the J_c values of melt processed samples reduced to much lower level than the required one when large magnetic fields were applied. In order to increase J_c even in magnetic fields, we need to introduce the pinning centers, which can prevent flux motion against the Lorentz force ($F_L = J \times B$) [9]. The resistive phase, which is commonly called green phase (as the color of this phase is green), or Y_2BaCuO_5 compound or 211-phase is appropriate to use as the pinning centers [10].

The correlation of J_c and microstructure of $YBa_2Cu_3O_{7-x}$ compound has been confirmed successfully by our group on the previously research [11]. In that research it was exhibited that the grain boundaries on the samples having a higher J_c are parallel to each other. It means that the grains were made to be alignment. Thus, the critical current density, J_c is strongly dependent on its microstructure. The question now is how the correlation between critical current density, J_c and lattice strain in $YBa_2Cu_3O_{7-x}$ compound. This physical phenomenon has never been investigated yet, so far. The aim of doing this research is to investigate the relation between the critical current density and the lattice strain in YBCO superconductor.

The microstructure of a crystal is characterized by its grains, i.e., size, shape, and grain-boundaries. The crystallite size is equivalent to the grain size if the individual grains are single crystals. The crystallite of a crystal is formed by the crystal unit cells. In this experiment, the size, shape, grain-boundaries, and grain orientation of a crystallite are changed by melt process. Consequently, the internal stresses and strains should be generated in the melt processed samples. As a hypothesis of this research is that the critical current density, J_c and the lattice strain in YBCO superconductor are inversely correlated, i.e. when the lattice strain decreases, critical current increases, and vice versa. It is because the critical current density, J_c and the weak links at the grain boundaries have an inversely correlation [8], while the lattice strains are directly correlated to the weak links.

THEORY

X-ray and neutron diffraction are powerful nondestructive techniques for characterizing latticestrain and/or stress in crystalline materials [12]. When a material is subject to a homogeneous strain field, the angular position of a diffraction peak will shift to lower or higher 2θ values, depending on whether the strain is tensile or compressive. If the materiasl is subject to an inhomogeneous strain field, then in addition to a peak position shift as mentioned above, the diffraction peak profile will also be broadened.

Thus, the shift of a peak measures the average lattice strain along a particular crystallographic direction. While, the peak broadening can be ascribed to either a small particle size or an inhomogeneous strain field, or both. Typically the broadening due to a small particle size appears in the form of a Lorentzian whereas that due the inhomogeneous strain field is described by a Gaussian function.

The profile shape function of a diffraction peak for each phase is a modified pseudo Voigt function, i.e. the sum of a Gauss function and a Lorentz function with unequal peak heights and full-widths at half maximum (FWHM):

$$g(2\theta_i - 2\theta_k) = \left(\frac{\gamma\pi^{1/2}H_k(G)}{c_0^{1/2}} + \frac{(1-\gamma)\pi H_k(G)}{c_1^{1/2}\delta}\right)^{-1} \times \left[\gamma \exp\left(\frac{-c_0(2\theta_i - 2\theta_k)^2}{H_k^2(G)}\right) + (1-\gamma)\left(1 + \frac{c_1(2\theta_i - 2\theta_k)^2\delta^2}{H_k^2(G)}\right)^{-1}\right] \quad \text{..... (1)}$$

where $2\theta_i$ is the scattering angle at the *i*th step, θ_k is the Bragg angle for the *k*th reflection, $C_0 = 4\ln 2$, $C_1 = 4$, γ is the Gaussian fraction, $\delta = H_k(G)/H_k(L)$, and $H_k(G)$ and $H_k(L)$ are the FWHMs of the Gaussian and Lorentzian components, respectively. $H_k(G)$ in Equation (1) is given by :

$$H_k(G) = U\tan^2\theta_k + V\tan\theta_k + W \quad \text{..... (2)}$$

where U, V, and W are the FWHM parameters. With appropriate choices of γ, the above profile shape function can vary from Gaussian ($\gamma = 1$) to Lorentzian ($\gamma = 0$). The differences between the pseudo Voigt function [13], and Equation (1) is that the value of δ is fixed at 1 in the former whereas δ is a variable parameter in the latter.

The Broadening of a Diffraction Peak Due to the Presence of an Inhomogeneous Strain Field is given by [14] :

$$B^2 = B_0^2 + 32\ln 2.\tan^2\theta.e_{hkl}^2 \quad \text{..... (3)}$$

Edisi Khusus Oktober 2007, hal : 46 - 52
ISSN : 1411-1098

where B is the FWHM of the broadened peak and B_0 is the instrumental resolution which varies with θ according to the Cagliotti equation [15] :

$$B_0^2 = U_0 \tan^2\theta + V_0 \tan\theta + W_0 \quad \text{..... (4)}$$

A simpler approach is taken to obtain an estimate of $< e >$, the average value of the anisotropic *rms* strains within the composites. Substituting Eq.(4) into Eq.(3), we have

$$B^2 = (U_0 + 32\ln 2. < e_{hkl}^2 >)\tan^2\theta + V_0 \tan\theta + W_0$$
$$= U \tan^2\theta + V_0 \tan\theta + W_0 \quad \text{..... (5)}$$

where $U = (U_0 + 32\ln 2. < e_{hkl}^2 >)$; so from this equation, we have

$$< e_{hkl}^2 >= \frac{U - U_0}{32\ln 2} \quad \text{..... (6)}$$

where U is the FWHM parameters of the broadened peak due to the presence of an inhomogeneous strain field and U_0 is the one due to the instrumental resolution only.

For precise strain measurements need a high angular resolution x-ray/neutron diffractometer. By using the Rietveld analysis method, the precision of the strain measurements can be further improved. In a Rietveld analysis, structure parameters calculated for every phases in a composite sample can be determined very accurate although there are many overlap reflections. In a Rietveld analysis, the parameters in a structural model, plus necessary instrumental parameters, are adjusted in a computer calculation until the least-squares best fit is obtained between the entire calculated and observed powder patterns.

Since a large number of diffraction peaks are fitted simultaneously, the statistical errors introduced in individual peak fitting are largely reduced. Moreover, by fitting to the whole pattern, any effects of preferred orientation, extinction, and other systematic aberrations, if present, will also be minimized [16]. Accordingly, the maximum amount of information can reliably be derived from the observed intensity data. Therefore, this technique has now found wide spread application in the structure determination of compounds which are not available as single crystals.

EXPERIMENTAL METHOD

Sample Preparation

A solid sintered $Y_1Ba_2Cu_3O_{7-x}$ superconductor (123-phase) were prepared in the same way as described in our earlier publication [17-19]. Figure 1 displays the heat treatment patterns followed in the present investigations. At high temperatures above 1200ºC, Y_2O_3 plus liquid L (L: a mixture of BaO and CuO) are stable. On cooling, these two phases react peritectically to produce Y_2BaCuO_5 (211-phase) :

$$Y_2O_3 + L(BaO+CuO) \rightarrow Y_2BaCuO_5.$$

At around 1000 ºC, 211-phase reacts with liquid L to produce 123-phase :

$$Y_2BaCuO_5 + L(3BaCuO_2 + 2CuO) \rightarrow 2Y_1Ba_2Cu_3O_{7-x}.$$

As shown at Figure 1, the samples were heated from room temperature (A point) to 1100ºC with the rate of 300ºC/h and hold at 1100ºC (BC segment) for t minute, and then rapidly cooled to 1000ºC (CD segment) with the rate of 400ºC/h. Subsequently samples were slowly cooled to 960ºC with the rate of 10-20ºC/h (DE segment), and then finally cooled to room temperature with the rate of 60ºC/h (EF segment). In this experiment, t parameters (BC segment) is made in variations, i.e. 1, 6, 12, and 18 minutes, accordingly we get four kinds of sample called YBCO-M1, YBCO-M6, YBCO-M12, and YBCO-M18, respectively, besides the one of sintered $Y_1Ba_2Cu_3O_{7-x}$ superconductor that called YBCO-S.

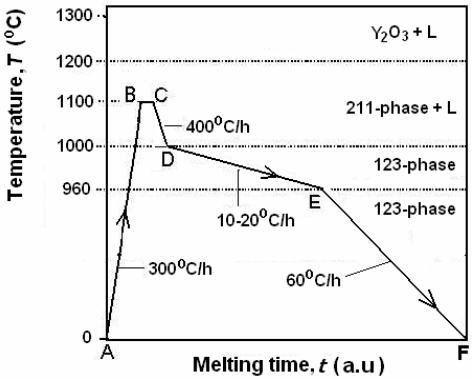

Figure 1. Schematic of the heat treatment pattern followed in samples preparation

Characterizations

The qualitatively and quantitatively phases analysis on YBCO-S, YBCO-M1, YBCO-M6, YBCO-M12, and YBCO-M18 samples were carried out by X-rays diffraction technique using the Rietveld method [20]. Rietveld method is the whole pattern fitting of calculated to observed powder patterns through least-squares refinement of model(s) for the structure(s), diffraction optics effects, and instrumental factors. The X-rays diffraction experiments were performed by using a Philips X-Ray Diffractometer, PW170 type. The X-ray intensity data from every point were collected at room temperature with CuKα radiation for 1 sec from 20° to about 80° in 2θ at a step size of 0.020°. Transport J_c measurements, were carried out by a standard four-probe method. The superconducting critical current density, J_c were determined using the relation:

$J_c = 0.318.I_c.s^{-2}$, where s = the distance between probe [cm], and I_c = the critical current [A] [21]. All of these experiments were carried out at Technology Centre for Nuclear Industry of Materials, Kawasan Puspiptek, Tangerang, Banten.

RESULT AND DISCUSSION

Figure 2 shows Rietveld refinement of YBCO-S sample. Its space group was assumed to be Pmmm (No. 47) and structural parameters obtained previously for orthorhombic YBCO [22] were used as initial values. Final crystal-structural parameters are listed in Table 1, and unit cell dimensions are listed in Table 2. In the upper portion of the figure here and elsewhere shows the observed data indicated by the dots; the calculated patterns is shown as the solid line overlying them. The vertical makers in the central portion show positions calculated for $K\alpha_1$ and $K\alpha_2$ peaks. The lower portion is plots of Δ, the difference between the observed and calculated intensities. On that figure is clearly showed that the full powder pattern calculated from the refined parameters matched the experimental pattern. These results support the ideas that YBCO-S sample does contain only 123-phase with the structural parameters as mentioned above. The YBCO-S sample were then separated into four same portions, and each of it is going to be melted with different melting time.

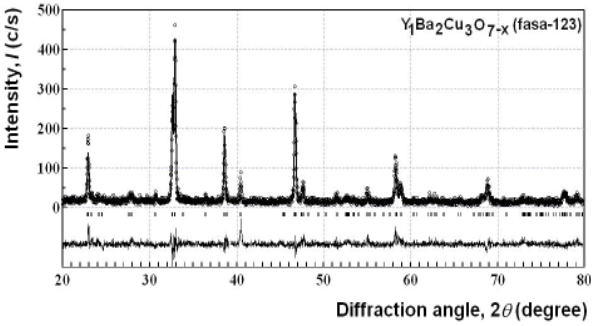

Figure 2. X-ray diffraction pattern of YBCO-S after being fitted by Rietveld analysis method.

Table 1. Crystal structural parameters in orthorhombic YBCO (123 phase). Throughout this paper, figures in parentheses are estimated standard deviation referring to the last digit

Atom / Site	*x*	*y*	*z*	*g*
Y	0.5	0.5	0.5	1.0
Ba	0.5	0.5	0.145(1)	0.42(2)
Cu(1)	0.0	0.0	0.0	1.0
Cu(2)	0.0	0.0	0.316(2)	1.0
O(1)	0.5	0.0	0.0	1.0
O(2)	0.0	0.5	0.0	0.01
O(3)	0.0	0.0	0.070(7)	1.0
O(4)	0.0	0.5	0.30(1)	1.0
O(5)	0.5	0.0	0.32(1)	1.0

Figure 3 shows Rietveld refinement of YBCO-M1 (a), YBCO-M6 (b), YBCO-M12 (c), and YBCO-M18 (d), where those samples actually ascribe to YBCO-S sample after being melted on 1100 °C for 1, 5, 12, and 18 minutes, respectively. According to the previous investigation [23] and theoretical background which have been mentioned above has been proven that in the melt-processed YBCO contain two phases, i.e. 123 phase and 211 phase. Therefore, Rietveld analysis of those samples were based on two space group: Pmmm (No. 47) for 123 phase and Pnma, (No. 62) for 211 phase. Structural parameters obtained previously for orthorhombic 123 phase [22] and tetragonal 211 phase [23] were used as initial values.

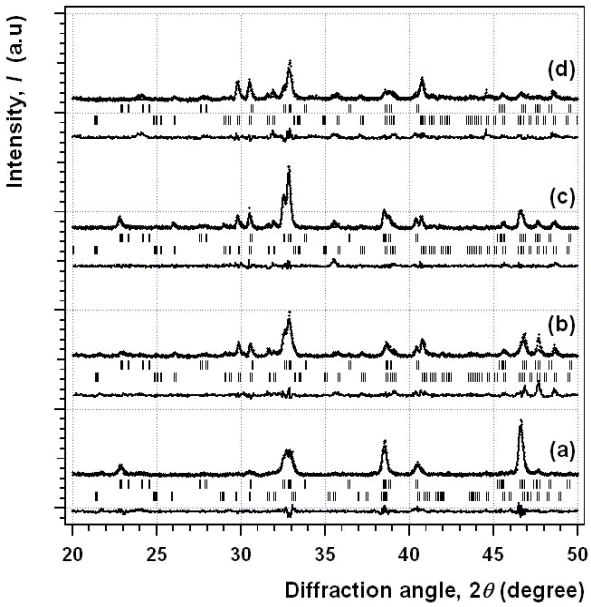

Figure 3. X-ray diffraction pattern after being fitted by Rietveld analysis method on the samples of YBCO-M1 (a), YBCO-M6 (b), YBCO-M12 (c), and YBCO-M18 (d).

Table 2. A listing of unit cell dimensions of 123 phase and 211 phase each in YBCO-S, YBCO-M1, YBCO-M6, YBCO-M12, and YBCO-M18 samples.

No.	Sample	123-phase			211-phase			
		a (Å)	*b* (Å)	*c* (Å)	*a* (Å)	*b* (Å)	*c* (Å)	*S* factors
1.	YBCO-S	3.888(1)	3.823(1)	11.685(3)	-	-	-	1.223
2.	YBCO-M1	3.886(3)	3.816(3)	11.696(8)	12.32(1)	5.596(8)	7.164(6)	1.264
3.	YBCO-M6	3.878(9)	3.815(8)	11.65(2)	12.17(2)	5.64(1)	7.12(1)	1.629
4.	YBCO-M12	3.880(3)	3.816(3)	11.69(1)	12.17(1)	5.654(5)	7.128(6)	1.297
5.	YBCO-M18	3.87(1)	3.81(1)	11.67(3)	12.18(3)	5.65(1)	7.12(2)	1.665

Table 3. Bragg angle (2 θ) data, and full width at half maximum (FWHM) of the three highest peaks in $Y_1Ba_2Cu_3O_{7-x}$ (123 phase) after being corrected by instrumental broadening.

No.	Sample	Bragg Angle (2θ) [º]			Full Width at Half Maximum (FWHM)[º]		
		(013)	(005)	(006)	(013)	(006)	(103)
1.	YBCO-S	32.770	38.456	46.556	0.054	0.003	0.055
2.	YBCO-M1	32.808	38.449	46.547	0.200	0.113	0.202
3.	YBCO-M6	32.875	38.591	46.723	0.134	0.135	0.134
4.	YBCO-M12	32.820	38.469	46.572	0.077	0.051	0.077
5.	YBCO-M18	32.848	38.510	46.623	0.106	0.131	0.106

Table 4. The phase quantity, average crystallite sizes, D, and lattice strains, <ehkl> in $YBa_2Cu_3O_{7-x}$ (123 phase).

No.	Sample	Phase quantity [wt%]		Average	Average
		123-phase	211-phase	Crystallite Sizes, D [Å]	Lattice Strains, $<e_{hkl}>$ [%]
1.	YBCO-S	100.00	0.00	9652	0.117
2.	YBCO-M1	83.41	16.59	571	0.103
3.	YBCO-M6	65.91	34.09	629	0.056
4.	YBCO-M12	73.83	26.17	1361	0.065
5.	YBCO-M18	47.64	52.36	729	0.061

As shown in Figure 3, the experimental data are plotted by dots, and the solid curve overlying the data dots is a diffraction pattern calculated from the final parameters. The Rietveld refinements converged most satisfactory, giving quite-low S factors (Table 2), where *S* is the goodness of fitting indicator. It means that the calculated patterns matched the experimental one. These results show that the samples just contain two phases, i.e. 123 phase and 211 phase. There are no other phases which may arise from the melt-process. Final unit cell dimensions are listed in Table 2. It is appeared in that table, that the lattice parameters of the two phases can be refined in such a way that they have an estimated standard deviation until 10^{-3} ú order.

On Table 3 are listed the Bragg angle (2θ) data, and full width at half maximum (FWHM) of the three highest peaks in 123 phase after being corrected by instrumental broadening. It is observed from that table, that the values of the angular position of diffraction peaks of the melt-processed samples shift to higher 2θ values referring to YBCO-S. It means that the melt processed samples undergo a compressive strain. This idea is supported by the fact that the 123 phase unit cell, especially *a*-, and *b* lattice, of melt-processed samples have a tendency to shorten referring to that of YBCO-S. While the *c*-lattice is relatively no change statistically referring to YBCO-S. From this facts be concluded that**,** the compressive strain occurs on the *a*-*b* plane of melt processed samples.

In addition, a little bit broadening of diffraction peak profile referring to that of YBCO-S occur on the melt-processed samples indicated by their FWHM. According to Xun-Li Wang *et al*. [24], the peak broadening can be ascribed to either a small particle size or an inhomogeneous strain field, or both. In this experiment, the most probable causes of peak broadening on the melt-processed samples are both of small particle size and inhomogeneous strain field. This conclusion is based on data on Table 2 and Table 4. The compressive strain just occurs on the basal plane and not in *c*-direction (Table 2); so it means that the strain is inhomogeneous. From data on Table 4, we can see that the crystallite sizes of melt-processed samples are getting smaller than the one of YBCO-S, where the crystallite sizes were determined by Scherrer equation [25]. Thus, it means that the particle size were reduced by melt process.

Figure 4 shows voltage-current characteristics on YBCO-S, YBCO-M1, YBCO-M6, YBCO-M12, and YBCO-M18 samples, with the critical current, I_c of 0.5, 10.93, 12.81, 17.02, and 8.53 A, respectively. These data reveal theirs meaning that when a current pass along the sample, then the voltage *V* develop between the ends varies as the magnitude *I* of the current is altered. So long as the current is less than the critical value I_c no voltage is observed along the sample, but when the current is increased above I_c a voltage appears which, at currents somewhat greater than I_c, approaches a linear increase with increasing current. The critical current densities were obtained through the relation of $J_c = 0.318.I_c.s\text{-}^2$, where s = the distance between probe [cm], and I_c = the critical current [A] as mentioned before [21]. The calculated J_c of YBCO-S, YBCO-M1, YBCO-M6, YBCO-M12, and YBCO-M18 samples are 3.98, 87.02, 101.99, 135.51, and 67.91 Acm^{-2}, respectively.

On Table 4 are listed the phase quantity, average crystallite sizes, and lattice strains in YBCO-S, YBCO-M1, YBCO-M6, YBCO-M12, and YBCO-M18 samples. It is observed from that table that, mass fraction of 123 phase in YBCO-S is 100 %. The quantity of

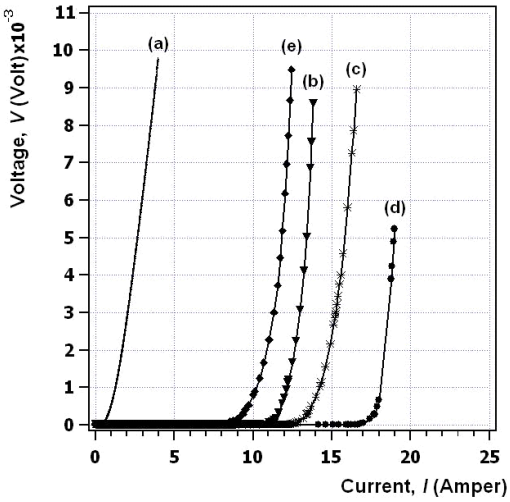

Figure 4. Voltage current characteristics on the samples of YBCO-S (a), YBCO-M1 (b), YBCO-M6 (c), YBCO-M12 (d), and YBCO-M18 (e).

123 phase becomes smaller with increasing melting time. It means that the longer the melting time, the more the quantity of 211 phase formed is, as shown in Figure 5(a). The lattice strains also becomes lower with increasing melting time but in a rather different way as shown in Figure 5(b), that is, in a parabolic curve. However, the lattice strains tend to increase again after the sample being melted for 18 minutes. Thus, there are some stress releases to some extents in YBCO with melt process. Accordingly, the lattice strain decreases with increasing the melting time.

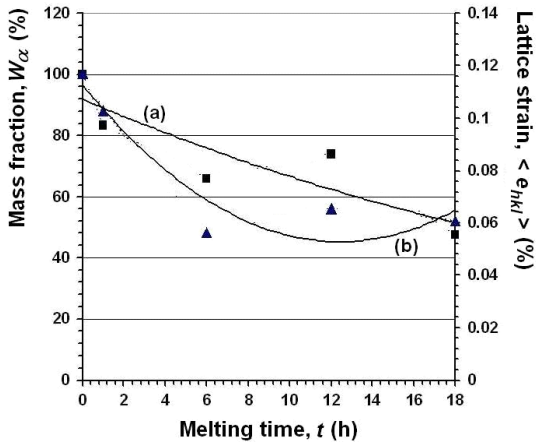

Figure 5. The curves of 123 phase mass fraction (a), and 123 phase lattice strain (b) each to the melting time.

Though, the critical current density, J_c and the lattice strain in YBCO superconductor have an inversed correlation, i.e. when the lattice strain decrease (Figure 6(a)), then critical current increase (Figure 6(b)), and vice versa. It is because the critical current density, J_c and the weak links at the grain boundaries have an inversely correlation [8], where the more the weak links at the grain boundaries reduced, the better the electrical contact

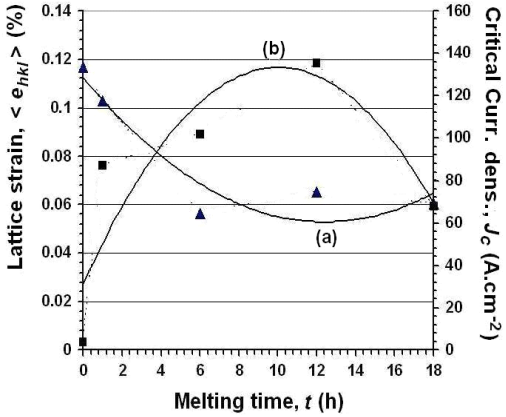

Figure 6. The curves of 123 phase lattice strain (a), and 123 phase critical current density (b) each to the melting time.

among the grains is, and so the J_c value become higher. The more the weak links at the grain boundaries reduced, the better the degree of grains alignment is. The better the degree of grains alignment, the more the lattice strain decreased is.

In this experiment is shown that the critical current densities, J_c continuously increase with increasing melting time until 12 minutes of melt process. The melt process through 12 minutes may have reduced the weak links. Therefore, the critical current density increases, and the lattice strain decreases. This finding is in agreement with the previously result reported by M. Murakami [26], where it was expressed that the melt process may have possibly eliminated the weak links and increases the critical current density.

CONCLUSIONS

Using the analysis methods outlined above, the influence of lattice strain to the critical current density of YBCO superconductor have been successfully determined. It have been successfully confirmed that YBCO produced by sintering method contain only 123 phase, and YBCO made by the melt process contain two phases, i.e. 123 phase and 211 phase. The critical current density and the lattice strain in YBCO superconductor are inversely correlated, i.e. when the lattice strain decreases, critical current increases, and vice versa. The critical current density increases or the lattice strain reduces with increasing melting time until 12 minutes of melt process.

This finding has confirmed that critical current density of YBCO superconductor can be increased by reducing the weak link at the grain boundary. Decreasing the weak link can be reached by making the grain alignment better. So, it means that the lattice strain can be decreased by making the grain alignment better.

Edisi Khusus Oktober 2007, hal : 46 - 52
ISSN : 1411-1098

ACKNOWLEDGEMENTS

We would like to thank to the Head of Technology Centre for Nuclear Industrial Material, Dr. Ridwan for his support of this research, and to the Head of Nuclear Analysis Division, Dr. Setyo Purwanto for his support; also our thanks to all of our colleagues on their helps. This project has been founded by DIPA-BATAN 2006.

REFERENCES

[1]. J.G. BEDNORZ, and K.A. MULLER, *Z. Physic* **B64**, (1986) 189
[2]. http://w3.infp.fzk.de:8080/extern/hotline/statusreport/sr98/preface.html, August 2, (1999)
[3]. M.K. WU, J. ASHBURN, C.J. TORNG, P.H. MENG, L. GAO, Z.J. HUANG, U.Q.WANG and C.W. CHU, *Phys. Rev. Lett.*, **58** (1987) 908
[4]. H. MAEDA, Y. TANAKA, M. FUKUTOMI and T. ASANO, *Jap. J. Appl. Phys*., **27** (1988) L209
[5]. Z.Z. SHENG and A.M. HERMAN, *Nature*, **332** (1988) 138
[6]. D.C. LARBALESTIER, *Physics Today*, **6** (1991) 74
[7]. D.C. LARBALESTIER, S.E. BABCOCK, X. CAI, M. DAEUMLING, D.P. HAMPSHIRE, T.F. KELLY, L.A. LAVANIER, P.J. LEE and J. SEUNTJENS, *Physica*, **C 153-155** (1988) 1580
[8]. ENGKIR SUKIRMAN, WISNU ARI ADI, dan SALMAH, Majalah BATAN, **XXXIII**(1/2) (2000) 31-45
[9]. M. MURAKAMI, M. MORITA, K. DOI and M. MIYAMOTO, *Jap. J. Appl. Phys*., **28** (1989) 1189
[10]. ENGKIR SUKIRMAN, WISNU ARI ADI, DIDIN S. WINATAPURA dan YUSTINUS, *Jurnal Ilmiah Teknik Mesin*, **8** (2) (2006) 79-90
[11]. ENGKIR SUKIRMAN, WISNU ARI ADI, dan SALMAH, *Majalah BATAN*, **XXXIII**(1/2) (2000) 31– 45
12]. D.S. KUPPERMAN, S. MAJUMDAR, and J.P. SINGH, *Neutron News*, **2** (3) (1991) 15-18
[13]. R.A. YOUNG and D.B. WILES, *J. Appl. Crystallogr*., **15** (1982) 430
[14]. H.P. KLUG and L.E. ALEXANDER, *X-ray Diffraction Procedures*, 2ND Ed.,Wiley, New York, (1974) 618-708
[15]. G. CAGLIOTTI, A. PAOLETTI, and F.P. RICCI, *Nuc. Instrum*., **3** (1958) 223-228
[16]. R.J. HILL and C.J. HOWARD, *J. Appl. Crystallogr*., **20** (1987) 467-474
[17]. DIDIN S. WINATAPURA, WISNU ARI ADI, GRACE TJ. SULUNGBUDI dan ENGKIR SUKIRMAN, *Prosiding Pertemuan Ilmiah IPTEK Bahan'02*, (2002) 168-172
[18]. ENGKIR SUKIRMAN, WISNU ARI ADI, DIDIN S. WINATAPURA dan YUSTINUS P., *Prosiding Pertemuan Ilmiah Iptek Bahan '04*, (2004) 233-240
[19]. DIDIN S. WINATAPURA, WISNU ARI ADI, dan ENGKIR SUKIRMAN**,** *Prosiding Pertemuan Ilmiah Iptek Bahan '04*, (2004) 287-292
[20]. F. IZUMI, *Rigaku J*., **6** (1089) 10
[21]. WISNU ARI ADI, ENGKIR SUKIRMAN, DIDIN S. WINATAPURA, GRACE TJ. SULUNGBUDI, *Majalah BATAN*, **XXXIV**(1/2) (2001) 15-30
[22]. ENGKIR SUKIRMAN, *Pengaruh Distribusi Kekosongan Oksigen pada Superkonduk- tivitas* $YBa_2Cu_3O_{7-x}$, *Tesis-S2*, Program Studi Materials Science, Fakultas Pascasarjana, Universitas Indonesia, (1991)
[23]. E. SUKIRMAN**,** WISNU ARI ADI, D. SAHIDIN WINATAPURA, dan SUPANDI, *Prosiding Seminar Nasional Hamburan Neutron dan Sinar-x Ke 5*, (2003) 112-116
[24]. XUN-LI WANG, CAMDEN R. HUBBARD, KATHLEEN B. ALEXANDER, PAUL F. BECHER, JAIME A. FERNANDEZ-BACA, and STEVE SPOONER, *J. Am. Ceram. Soc*., **77**(6) (1994) 1569-1575
[25]. http://amialabs.com/AppNoteC02.swf, 26 June 2006
[26]. M. MURAKAMI, *Supercond. Sci*., **5** (1992) 185-203